

1 **Title:**

2 **Expression dynamics of ARGONAUTE proteins during meiosis in Arabidopsis**

3

4 **Authors and affiliation:**

5 Cecilia Oliver and German Martinez.

6 Department of Plant Biology, Uppsala BioCenter, Swedish University of Agricultural

7 Sciences and Linnean Center for Plant Biology, Uppsala, Sweden

8

9 **Corresponding authors:**

10 Cecilia Oliver: [cecilia.oliver.velasco@slu.se](mailto:cecilia.oliver.velasco@slu.se)

11 German Martinez: [german.martinez.arias@slu.se](mailto:german.martinez.arias@slu.se)

12

13 **ORCID information:**

14 Cecilia Oliver: 0000-0002-5231-7910

15 German Martinez: 0000-0002-5215-0866

## 16 **Abstract**

17 Meiosis is a specialized cell division that is key for reproduction and genetic diversity in  
18 sexually reproducing plants. Recently, different RNA silencing pathways have been  
19 proposed to carry a specific activity during meiosis, but the pathways involved during this  
20 process remain unclear. Here, we explored the subcellular localization of different  
21 ARGONAUTE (AGO) proteins, the main effectors of RNA silencing, during male meiosis  
22 in *Arabidopsis thaliana* using immunolocalizations with commercially available antibodies.  
23 We detected the presence of AGO proteins associated with posttranscriptional gene  
24 silencing (AGO1, 2 and 5) in the cytoplasm or the nucleus, while AGOs associated with  
25 transcriptional gene silencing (AGO4 and 9) localized exclusively in the nucleus. These  
26 results indicate that the localization of different AGOs correlates with their predicted roles  
27 at the transcriptional and posttranscriptional levels and provide an overview of their timing  
28 and potential role during meiosis.

29

## 30 **Introduction**

31 Meiosis is a special type of cell division where one round of DNA synthesis is followed by  
32 two rounds of cell division, segregating homologous chromosomes during the first division  
33 and sister chromatids at the second division (Marston et al. 2004, Mercier et al. 2015).  
34 This process is key for the production of gametes and the reshuffling of the genetic  
35 information during sexual reproduction (Bolcun-Filas et al. 2018). The mechanisms  
36 regulating meiosis have been widely studied at the cellular, genetic, and molecular levels  
37 in a variety of organisms. In plants, more than 90 genes have been identified comprising

38 different meiotic processes that include double-strand break (DSB) formation,  
39 chromosome segregation or meiotic recombination (Huang et al. 2019a). Intriguingly, in  
40 the recent years it has been revealed that several of these processes involve the RNA  
41 silencing machinery (Oliver et al. 2016, Underwood et al. 2018, Wei et al. 2012). Different  
42 RNA silencing pathways are active during meiosis (Huang et al. 2020, Huang, et al.  
43 2019a, Yelina et al. 2015). The miRNA affects chromatin condensation and the number  
44 of chiasmata, while the RNA-directed DNA methylation (RdDM) pathway affects  
45 chromatin condensation, the number of chiasmata and chromosome segregation (Oliver  
46 et al. 2017, Oliver, et al. 2016). Moreover, the RdDM pathway protects euchromatic  
47 regions from meiotic recombination (Yelina, et al. 2015). Additionally, *Arabidopsis* a non-  
48 canonical RNA silencing pathway plays a role in double-strand break repair (Wei, et al.  
49 2012). Moreover, meicyte-specific sRNAs between 23-24 nts are positively correlated  
50 with genes that have a meicyte-preferential expression pattern (Huang, et al. 2019a),  
51 which could correlate with the observed role of DNA methylation in the regulation of gene  
52 expression in meicytes (Walker et al. 2018). ARGONAUTE (AGO) proteins are the  
53 effectors of the different RNA silencing pathways and have dedicated members that act  
54 at the posttranscriptional or transcriptional levels. Here, we analyze the subcellular  
55 localization of the main AGO proteins in *Arabidopsis* during the different meiosis stages,  
56 which provides a confirmation of their activity during this process.

57

## 58 **Materials and Methods**

59

### 60 **Plant material**

61 Plants used for immunolocalization analysis were grown in a phytotron under long day  
62 conditions (16-hour light/8-hour dark photoperiod), at 24-25 °C and 45% relative humidity.

63

#### 64 **Bioinformatic analysis**

65 sRNA data was downloaded from the SRA repository project number PRJNA510650  
66 (Huang et al. 2019b). sRNA alignments were performed using bowtie (Langmead et al.  
67 2009) with the following parameters `-t -v2` that allows 2 mismatches to the alignments.  
68 For sRNA categorization a miRNAs, sRNA libraries were aligned to individual indexes  
69 generated for each genomic category and compared total sRNAs mapping to the TAIR10  
70 chromosome sequences. Transcriptomic data corresponds to the ATH1 data from  
71 GSE10229 and GSE13000 (Libeau et al. 2011) and data extracted using the CATdb  
72 database ([http://urgv.evry.inra.fr/cgi-bin/projects/CATdb/catdb\\_index.pl](http://urgv.evry.inra.fr/cgi-bin/projects/CATdb/catdb_index.pl)).

73

#### 74 **Cytology:**

75 Immunolocalization on meiotic nuclei were carried out by squash technique as was  
76 previously described by Manzanero et al. (2000) with some modifications (Oliver et al.,  
77 2013). Two bioreplicates of young buds from five plants each, were analyzed. The primary  
78 antibodies used were rabbit anti-AGO1 (1:200 AS09 527), -AGO2 (1:100, AS13 2682), -  
79 AGO5 (1:100, AS10 671), -AGO4 (1:100, AS09 617), -AGO6 (1:50, AS10 672), -AGO9  
80 (1:100, AS10 673) and -AGO10 (1:50, AS15 3071) antibodies from Agrisera. Secondary  
81 antibody used was goat anti-rabbit IgG H&L Alexa Fluor 568 conjugated (1:200;  
82 ab175471; Abcam). The slides were stained with the DAPI, 1 µg/ml during 20-30 min and  
83 finally mounting with antifading medium (0.2% n-propyl Galleate, 0.1% DMSO, 90%  
84 glycerol in PBS). Fluorescent signals were observed using an epifluorescence  
85 microscope Zeiss Axio Scope A1. Images were captured with AxioCam ICc5 camera and  
86 were analyzed and processed with ImageJ and Affinity Photo software.

87

#### 88 **Results**

89 To discern the level of expression of RNA silencing components in meiocytes, we  
90 analyzed their expression from publicly available microarray datasets (Libeau, et al. 2011)  
91 (Figure 1 and Supplementary Methods). Overall, several components from the RNA  
92 silencing pathways were preferentially expressed in meiocytes compared to somatic  
93 tissues (Figure 1A), including the AGO proteins AGO4, 5 and 10, the Dicer-like (DCL)  
94 proteins DCL1, 3 and 4 or the sRNA methyltransferase HEN1. This indicated that different  
95 PTGS (AGO5, DCL1 and DCL4) and TGS (AGO4 and DCL3) pathways might be  
96 especially active during meiosis. Previous analysis (Huang, et al. 2019a) have shown that  
97 TE-derived sRNAs accumulate to relatively high levels in meiocytes and that certain  
98 miRNAs like miR845 are active before the microspore stage (Borges et al. 2018).  
99 Although miRNAs were not globally enriched in meiocytes (Figure 1B), several miRNAs  
100 were strongly upregulated including miR839, miR780.2, miR780.1, miR157, miR172,  
101 miR166 and miR860, which are important regulators of several transcription factor  
102 families (Figure 1C, Supplementary Figure 1 and Supplementary Table 2). In summary,  
103 transcriptomic and sRNA sequencing analysis supported the notion that the RNA  
104 silencing machinery might have a meiocyte-specific activity.

105

106 Although transcriptomic analysis is important to infer the activity of the different RNA  
107 silencing pathways in meiocytes, this analysis provides a steady image of this tissue and  
108 ignores, for example, its dynamism during meiosis. To understand the subcellular  
109 localization and dynamics of the different AGO proteins during meiosis, we performed  
110 immunolocalizations of the AGO proteins that had commercially available antibodies  
111 (Agrisera, AGO1, 2, 4, 5, 6, 9 and 10, Figure 2 and Supplementary Methods). During

112 meiosis all AGOs but AGO6 and AGO10 could be detected. In detail, AGO1 and its  
113 paralogs AGO2 and AGO5 displayed a similar localization and expression pattern during  
114 the first meiotic stages (Figure 2A, 2B, 2C). The three proteins were located mainly in the  
115 cytoplasm, similar to their localization in somatic tissues (Bologna et al. 2018, Ye et al.  
116 2012). From the leptotene to the diplotene stage these three AGO proteins formed  
117 cytoplasmic granules (Figure. 2A1, 2B1, 2C1). In somatic tissues, cytoplasmic bodies are  
118 involved in the degradation and translation arrest of mRNAs (Maldonado-Bonilla 2014).  
119 In mammals, AGO proteins localize in P-bodies where they mediate the translational  
120 repression of their target mRNAs (Liu et al. 2005). The localization pattern observed for  
121 AGO1, 2 and 5 might indicate a similar role of RNA silencing in the posttranscriptional  
122 regulation of mRNAs, a process that is known to take place in other organisms like  
123 mammals (Yao et al. 2015).

124

125 Despite the similarities between the accumulation during meiosis, AGO1, 2 and 5, they  
126 showed differences in their dynamics during meiosis. For example, AGO1 condensates  
127 around the nuclear envelope at diplotene (Figure 2A4) but after this stage, it showed a  
128 disperse accumulation (Figure 2A5). This location during cell division could be related  
129 with the known AGO1 association with the endoplasmic reticulum (Li et al. 2013), as when  
130 the nuclear envelope disassembles it reorganizes in vacuoles around the bivalents  
131 (Marston, et al. 2004, Mercier, et al. 2015). AGO5 displayed a similar pattern of  
132 subcellular localization to AGO1, although its localization at cytoplasmic bodies  
133 disappeared at diplotene (Figure 2B4). On the other hand, AGO2 showed a dual  
134 localization in the cytoplasm and in the nucleus (Figure 2C1-4) and was not detectable

135 after metaphase I (Figure 2C5-6). Both its nucleocytoplasmic localization and timing of  
136 expression are in line with its known role in double strand break (DSB) repair, which takes  
137 place during the first meiotic stages (Oliver et al. 2014, Wei, et al. 2012). Nevertheless,  
138 AGO2 expression pattern was recapitulated after the second meiotic division (Figure  
139 2C7), indicating that it might serve other roles in parallel to its function in DSB repair  
140 during meiosis.

141

142 On the other hand, the TGS/RdDM-associated AGO proteins, AGO4 and AGO9, were  
143 located in the nuclei during all meiotic stages (Figure 2D and E). Exceptionally, at  
144 metaphase I, when the nuclear envelope dissolves, both proteins showed a dispersed  
145 accumulation. This is in accordance with the known role of the RdDM pathway in  
146 regulating DNA methylation during meiosis (Walker, et al. 2018). Meiocytes have the  
147 lowest CHH methylation values of all the reproductive nuclei analyzed, but its activity is  
148 needed for the regulation of gene expression (Walker, et al. 2018). We detected a low  
149 accumulation of AGO4 and 9 after metaphase I (Figure 2D5-6 and 2E5-6), which might  
150 partially cause this reduction in CHH methylation. Interestingly, we observed that AGO9  
151 displayed a localization pattern compatible with a preference for heterochromatic regions  
152 at pachytene. This localization might explain the known role of AGO9 on the dissolution  
153 of interlocks during meiosis (Oliver, et al. 2014).

154

155 **Discussion**

156 In summary, our results provide an overview of the subcellular localization, timing and  
157 potential role of different RNA silencing pathways during meiosis. Furthermore, our work  
158 complements previous analysis that analyzed RNA silencing activity in meiocytes, and  
159 opens the door for future molecular analysis of the specific role of AGO proteins during  
160 specific meiosis stages, which are technically challenging at the moment.

161

162 **Author contribution statement:** C.O and G.M. design the experiments and wrote the  
163 manuscript. C.O. performed the experiments and analyzed the data. G.M. analyzed the  
164 bioinformatic data.

165

## 166 **Acknowledgements**

167 The authors thank SLU, the Carl Tryggers Foundation (CTS 17-305 and CTS 18-251),  
168 the Swedish Research Council (VR 2016-05410) and the Knut and Alice Wallenberg  
169 Foundation (KAW 2019-0062) for supporting research in the Martinez group. The data  
170 handling was enabled by resources provided by the Swedish National Infrastructure for  
171 Computing (SNIC) at UPPMAX partially funded by the Swedish Research Council through  
172 grant agreement no. 2018-05973.

173

## 174 **References:**

175 Bolcun-Filas E, Handel MA (2018) Meiosis: the chromosomal foundation of reproduction.  
176 Biol Reprod 99:112-126



177 Bologna NG, Iselin R, Abriata LA, Sarazin A, Pumplin N, Jay F, Grentzinger T, Dal Peraro  
178 M, Voinnet O (2018) Nucleo-cytosolic Shuttling of ARGONAUTE1 Prompts a  
179 Revised Model of the Plant MicroRNA Pathway. *Mol Cell* 69:709-719 e705

180 Borges F, Parent JS, van Ex F, Wolff P, Martinez G, Kohler C, Martienssen RA (2018)  
181 Transposon-derived small RNAs triggered by miR845 mediate genome dosage  
182 response in Arabidopsis. *Nat Genet* 50:186-192

183 Huang J, Wang C, Li X, Fang X, Huang N, Wang Y, Ma H, Wang Y, Copenhaver GP  
184 (2020) Conservation and Divergence in the Meiocyte sRNAomes of Arabidopsis,  
185 Soybean, and Cucumber. *Plant Physiol* 182:301-317

186 Huang J, Wang C, Wang H, Lu P, Zheng B, Ma H, Copenhaver GP, Wang Y (2019a)  
187 Meiocyte-Specific and AtSPO11-1-Dependent Small RNAs and Their Association  
188 with Meiotic Gene Expression and Recombination. *Plant Cell* 31:444-464

189 Huang JY, Wang C, Wang HF, Lu PL, Zheng BL, Ma H, Copenhaver GP, Wang YX  
190 (2019b) Meiocyte-Specific and AtSPO11-1-Dependent Small RNAs and Their  
191 Association with Meiotic Gene Expression and Recombination. *Plant Cell* 31:444-  
192 464

193 Langmead B, Trapnell C, Pop M, Salzberg SL (2009) Ultrafast and memory-efficient  
194 alignment of short DNA sequences to the human genome. *Genome Biol* 10:R25

195 Li S, Liu L, Zhuang X, Yu Y, Liu X, Cui X, Ji L, Pan Z, Cao X, Mo B, Zhang F, Raikhel N,  
196 Jiang L, Chen X (2013) MicroRNAs inhibit the translation of target mRNAs on the  
197 endoplasmic reticulum in Arabidopsis. *Cell* 153:562-574

- 198 Libeau P, Durandet M, Granier F, Marquis C, Berthome R, Renou JP, Taconnat-Soubirou  
199 L, Horlow C (2011) Gene expression profiling of Arabidopsis meiocytes. *Plant Biol*  
200 (Stuttg) 13:784-793
- 201 Liu J, Valencia-Sanchez MA, Hannon GJ, Parker R (2005) MicroRNA-dependent  
202 localization of targeted mRNAs to mammalian P-bodies. *Nat Cell Biol* 7:719-723
- 203 Maldonado-Bonilla LD (2014) Composition and function of P bodies in Arabidopsis  
204 thaliana. *Front Plant Sci* 5:201
- 205 Marston AL, Amon A (2004) Meiosis: cell-cycle controls shuffle and deal. *Nat Rev Mol*  
206 *Cell Biol* 5:983-997
- 207 Mercier R, Mezard C, Jenczewski E, Macaisne N, Grelon M (2015) The molecular biology  
208 of meiosis in plants. *Annu Rev Plant Biol* 66:297-327
- 209 Oliver C, Pradillo M, Jover-Gil S, Cunado N, Ponce MR, Santos JL (2017) Loss of function  
210 of Arabidopsis microRNA-machinery genes impairs fertility, and has effects on  
211 homologous recombination and meiotic chromatin dynamics. *Sci Rep* 7:9280
- 212 Oliver C, Santos JL, Pradillo M (2014) On the role of some ARGONAUTE proteins in  
213 meiosis and DNA repair in Arabidopsis thaliana. *Frontiers in Plant Science* 5
- 214 Oliver C, Santos JL, Pradillo M (2016) Accurate Chromosome Segregation at First Meiotic  
215 Division Requires AGO4, a Protein Involved in RNA-Dependent DNA Methylation  
216 in Arabidopsis thaliana. *Genetics* 204:543-553
- 217 Underwood CJ, Choi K, Lambing C, Zhao X, Serra H, Borges F, Simorowski J, Ernst E,  
218 Jacob Y, Henderson IR, Martienssen RA (2018) Epigenetic activation of meiotic  
219 recombination near Arabidopsis thaliana centromeres via loss of H3K9me2 and  
220 non-CG DNA methylation. *Genome Res* 28:519-531

221 Walker J, Gao H, Zhang J, Aldridge B, Vickers M, Higgins JD, Feng X (2018) Sexual-  
222 lineage-specific DNA methylation regulates meiosis in Arabidopsis. *Nat Genet*  
223 50:130-137

224 Wei W, Ba Z, Gao M, Wu Y, Ma Y, Amiard S, White CI, Rendtlew Danielsen JM, Yang  
225 YG, Qi Y (2012) A role for small RNAs in DNA double-strand break repair. *Cell*  
226 149:101-112

227 Yao CC, Liu Y, Sun M, Niu MH, Yuan QQ, Hai YA, Guo Y, Chen Z, Hou JM, Liu Y, He ZP  
228 (2015) MicroRNAs and DNA methylation as epigenetic regulators of mitosis,  
229 meiosis and spermiogenesis. *Reproduction* 150:R25-R34

230 Ye R, Wang W, Iki T, Liu C, Wu Y, Ishikawa M, Zhou X, Qi Y (2012) Cytoplasmic assembly  
231 and selective nuclear import of Arabidopsis Argonaute4/siRNA complexes. *Mol*  
232 *Cell* 46:859-870

233 Yelina NE, Lambing C, Hardcastle TJ, Zhao X, Santos B, Henderson IR (2015) DNA  
234 methylation epigenetically silences crossover hot spots and controls chromosomal  
235 domains of meiotic recombination in Arabidopsis. *Genes Dev* 29:2183-2202

236

## 237 **Figure legends:**

238 **Figure 1. Analysis of the expression in meiocytes of different RNA silencing and**  
239 **epigenetic pathways components and analysis of miRNA accumulation in**  
240 **meiocytes. A.** Heat map of the expression values of RNA silencing and epigenetic  
241 pathways components in meiocyte microarray experiments. Expression values are  
242 represented as the normalized log<sub>2</sub> ratio of the comparison meiocyte/control tissue. **B.**  
243 Global accumulation of miRNAs in leaves and meiocytes samples from public datasets

244 normalized to reads per million. **C.** Accumulation values of miRNAs enriched in meiocyte  
245 sRNA libraries. Enrichment was considered only for miRNAs accumulating more than 2-  
246 fold in meiocytes and with a p-value<0.05.

247

248 **Figure 2. Immunolocalization of AGO1 (A), AGO5 (B), AGO2 (C), AGO4 (D) and**  
249 **AGO9 (E) at different representative meiotic stages in Arabidopsis meiocytes.**  
250 Leptotene (A1, B1, C1, D1, E1); Zygotene (A2, B2, C2, D2, E2); Pachytene (A3, B3, C3,  
251 D3, E3); Diplotene (A4, B4, C4, D4, E4); Diakinesis (B5), Metaphase I (A5, C5, D5, E5)  
252 Prophase II (A6, B6, D6, E6); Metaphase II (C6); Tetrad (A7, B7, C7, D7, E7).  
253 Immunostaining with antibodies is shown in red, counterstaining with DAPI is shown in  
254 grey. Bar indicates 10  $\mu$ m.

255

256 **Supplementary Figure 1.** Predicted and confirmed targets of miRNA families  
257 significantly upregulated in meiocytes.

258

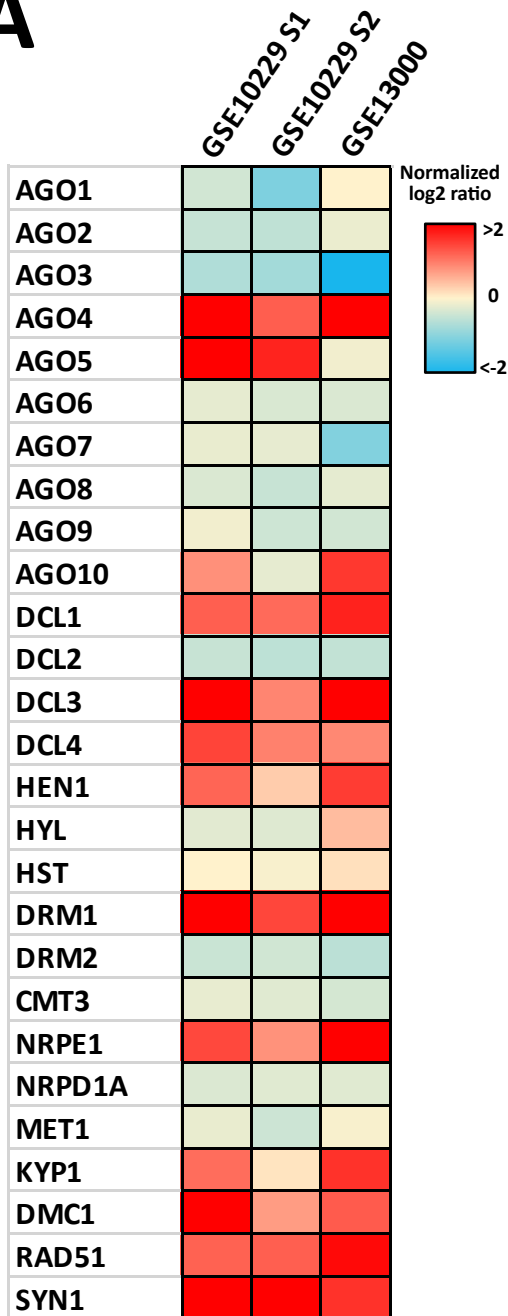
259 **Supplementary Table 1.** Raw values of normalized log2-ratio expression values for  
260 selected genes in meiocytes microarray data.

261

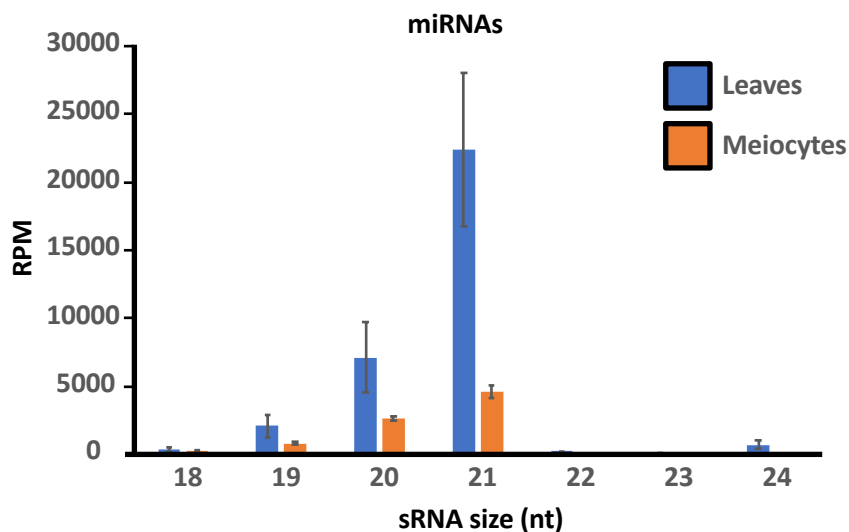
262 **Supplementary Table 2.** Raw values of miRNA accumulation in meiocytes and leaf  
263 sRNA libraries.

# Figure 1

## A



## B



## C

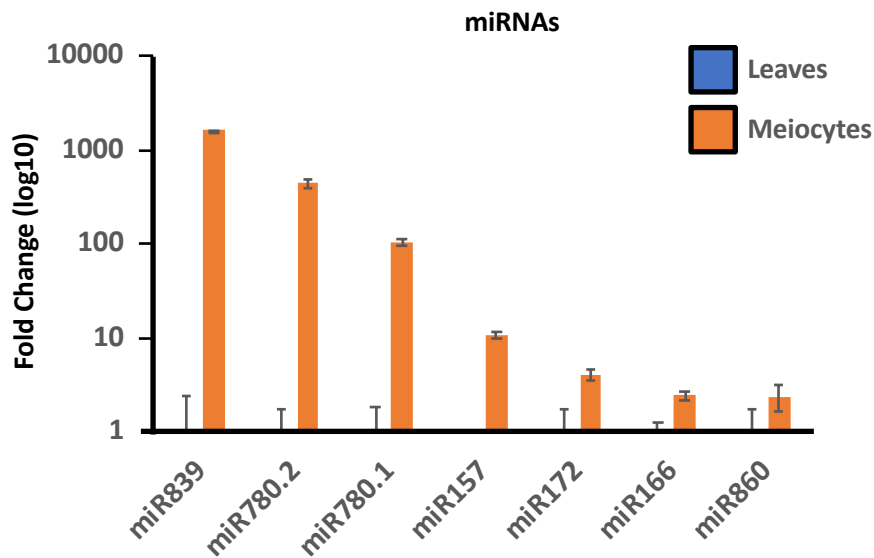


# Figure 2.

